Intelligent Automation And Soft Computing, 2018
Copyright © 2018, TSI® Press
Vol.24,no.3,571–580

Kinematic Calibration of a Parallel Manipulator for a Semi-physical Simulation System

Dayong Yu

School of Mechanical Engineering, University of Shanghai for Science and Technology, Shanghai, China

ABSTRACT

In the application of a semi-physical simulation system of a space docking mechanism, the simulation precision is determined by pose accuracy of the parallel manipulator. In order to improve pose accuracy, an effective kinematic calibration method is presented to enable the full set of kinematic parameter errors to be estimated by measuring the docking mechanism's poses. A new calibration model that takes into account geometrical parameter errors and coordinates transformation errors is derived by using a differential geometry method. Based on the calibration model, an iterative least square algorithm is utilized to calculate the above errors. Simulation and experimental results show the calibration method can obviously improve pose accuracy.

KEY WORDS: Kinematic calibration, Error modeling, Error compensation, Parameter identification, Parallel manipulator

1 INTRODUCTION

OVER the last five decades, parallel manipulators have been extensively researched for their some advantages of high rigidity, high accuracy, and high load-carrying capacity, and their general applications in motion simulators, parallel robots, and parallel machine tools etc. (Yao, et.al. 2016) (Yang, et.al. 2014) (Yang, et.al. 2012) (Sun, et.al. 2016) (Bernhard, et.al. 2001). Parallel manipulators can be used to simulate the relative motion between target spacecraft and tracking spacecraft in a semi-physical simulation system of a space docking mechanism by installing a space docking mechanism to the mobile platform. A semi-physical simulation system of a space docking mechanism has been constructed in the Aerospace System Engineering Shanghai in the 921 Manned Space project with Harbin Institute of Technology.

One of the important issues in applying the semi-physical simulation system of a space docking mechanism is pose accuracy of the parallel manipulator. The investigation of pose accuracy for parallel manipulators is mainly divided into two parts. One is accuracy analysis (Wang & Ehmann, 2002) (Ryu & Cha, 2003), and the other is kinematic calibration (Verner, et.al. 2003) (Li, et.al. 2017) (Bai & Teo, 2003). Accuracy analysis is defined as statistical analysis of the effects of manufacturing errors and installing errors on pose errors of parallel manipulators. Sensitivity analysis is used to modify the relevant error parameters to achieve the desired pose accuracy. In the aspect of accuracy analysis, an error model of a Stewart platform was built using D-H matrix theory, considering the manufacturing errors, installing errors and measuring errors. The error analysis results showed that the maximum errors for Stewart platforms occurred in the edge of the work space (Wang & Masory, 1993). A pose error formula of the moving platform was established by differentiating the inverse equation of Stewart platforms. The influence of the length errors of the drive rod and the position error of the hinge on the pose of the moving platform was analyzed (Ropponen & Arai, 1995). For the Stewart platform, an error model for pose accuracy synthesis analysis was established, and an analytic solution for the accuracy analysis of individual components has been given in this article. A pose error model of parallel manipulators was set up, and the pose error spatial distributions in a given work space were obtained by using a Sobol sequence based quasi-Monte Carlo method. This approach can significantly enhance evaluative precision of pose errors and reduce computational burden. According to the above information, the comparison of various design schemes in the stage can be carried on and the best scheme can be found through the accuracy analysis and accuracy synthesis (Li, et.al. 2015). It can also

CONTACT Dayong Yu yudayong_USST@163.com

calculate the influence of an original error on the pose accuracy. Thus, the key segments in parallel manipulators can be discovered, and the key points and directions to improve pose accuracy can be clearly defined. It can provide accurate and reliable information in order to improve design quality and design level of parallel manipulators.

Compared with accuracy analysis, kinematic calibration is the effective technique to solve the pose accuracy problem in the case that manufacturing and installing accuracy cannot be guaranteed. Pose accuracy can be improved without changing the hardware mechanism. A large number of investigations show that kinematic calibration is the most economical and feasible technologies to improve pose accuracy. The basic principle of kinematic calibration is that an error function between measured poses and calculated poses by using the kinematic model is constructed based on constraint and pose error observability. The kinematic parameters are identified by linear or nonlinear least square technique, and the inverse model parameters in the controller are corrected by the identification results, so as to achieve the goal of accuracy compensation. In general, kinematic calibration includes error modeling, pose measurement, error parameter identification and error compensation (Daney, 2003) (Zhuang & Roth, 1995). According to the different pose measurement technologies, calibration methods can usually be divided into external calibration (Takeda, et.al. 2004) (Renaud, et.al. 2006) (Tian, et.al. 2016) and self-calibration (Patel & Ehmann, 2000) (Ren, et.al. 2009). When the pose of parallel manipulators is completely measured, the inverse kinematic model can be used to solve the calibration problem. Since the pose information is partially measured, the calibration problem can only be solved by using the forward kinematic model. The calculation of external calibration based on complete pose measurement is more accurate, and the kinematic parameter identification performance is better because the inverse kinematics of parallel manipulators has analytic solutions. The forward kinematics of the parallel manipulators can usually obtain numerical solutions, so the calibration performance based on partial pose is relatively weak (Rauf, et.al. 2006). In order to ensure the calibration results, most of the external calibration based on the complete pose is used to identify all independent parameters of the model. Kinematic calibration of Stewart platforms was simulated and analyzed by using calibration technology of serial manipulators. The results show that the errors are reduced by an order of magnitude after kinematic calibration, but did not consider the influence of measurement error on calibration results (Masory, et.al. 1993). A simple calibration method was presented to identify a fixed leg length by changing other leg lengths. Kinematic parameters of each leg can be estimated separately, thereby the amount of calculation is reduced greatly. But this method has decreased the measurable work space (Zhuang & Yan, 1998). A calibration of parallel robots was proposed by using a tilt sensor. The effect of the tilt sensor noise and pose measurement number on kinematic calibration was simulated, but this method can only identify some parameters (Besnard & Khalil, 1999).

A kinematic calibration technique considering geometrical parameter errors of parallel manipulators, transformation errors between the docking coordinate frame and the mobile coordinate frame, and transformation errors between the fixed coordinate frame and the world coordinate frame is presented in order to solve simulation precision for a semi-physical simulation system of a spacecraft docking mechanism. In Section 1, the investigation on accuracy analysis and kinematic calibration is outlined, and its importance is pointed out. The article is organized as follows: The inverse kinematics and pose error model are given in Section 2. A kinematic calibration model containing the above errors is established by using the matrix differential theory, and an error parameter identification algorithm is developed based on iterative least squares in Section 3. In Section 4, the feasibility for the kinematic calibration technique is verified by computer simulation, and some experimental results are presented to further confirm the effectiveness of this technology. Section 5 concludes this paper.

2 KINEMATIC MODEL OF THE PARALLEL MANIPULATOR

THE parallel manipulator with a docking mechanism installed to its mobile platform is composed of six identical electro-hydraulic actuators connecting a mobile platform to a base platform with Hooke joints in parallel shown in Figure 1. The parallel manipulator can be simplified as a model shown in Figure 2(a). Two coordinate frames are established for the parallel manipulator. The fixed coordinate frame {B} is located in the center of the base platform. The mobile coordinate frame {A} is located in the center of the mobile platform. l_i (i=1,…,6) is the ith actuator length, a_i (i=1,…,6) represents upper joint coordinates in the mobile coordinate frame {A}, b_i (i=1,…,6) is the lower joint coordinates in the fixed coordinate frame {B}. The docking coordinate frame {D} is attached to the docking mechanism, and the world coordinate frame {W} is a unified reference frame as shown in Figure 2(b).

The homogeneous transformation matrix is used to express the pose of the coordinate frame {D} with respect to the world coordinate frame {W}, namely

$$\mathbf{T}_D^W = \mathbf{T}_B^W \mathbf{T}_A^B \mathbf{T}_D^A \tag{1}$$

2.1 *Inverse Kinematics*

The inverse kinematics can deal with the actuator lengths corresponding to a set of given poses of parallel manipulators and the kinematic parameters. The actuator lengths are calculated in the form of closed form solutions through analytic method.

The vector loop in Figure 2(a) can be expressed as

$$\mathbf{l}_i = \mathbf{R}\cdot\mathbf{a}_i + \mathbf{t} - \mathbf{b}_i \quad i = 1,2,\ldots,6 \tag{2}$$

The actuator length can be determined by calculating the norm of Eq. (2).

$$\|\mathbf{l}_i\| = \|\mathbf{R}\cdot\mathbf{a}_i + \mathbf{t} - \mathbf{b}_i\| \quad i = 1,2,\ldots,6 \tag{3}$$

Figure 1. **The Parallel Manipulator Constructed for the Space Docking Motion Simulation.**

2.2 *Error Model*

A pose error model of the parallel manipulator will relate the geometrical errors resulting from the manufacturing and assembly of the mobile platform and the base platform to the pose error of its mobile platform. To derive the pose error model, Eq. (2) is performed. The following differentiation is given below

$$\delta L_i\mathbf{u}_i + L_i\delta\mathbf{u}_i = \delta\mathbf{R}\cdot\mathbf{a}_i + \mathbf{R}\delta\mathbf{a}_i + \delta\mathbf{t} - \delta\mathbf{b}_i \tag{4}$$

Where L_i is the actuator length and $\mathbf{u}_i$ is the unit vector of the actuator. Because the rotation matrix $\mathbf{R}$ is orthogonal, it can be expressed as

$$\delta\mathbf{R} = \mathbf{\Omega}\mathbf{R} \tag{5}$$

Where $\mathbf{\Omega}$ is a 3×3 skew symmetric matrix whose nonzero element represents the orientation error $\delta\boldsymbol{\omega}$ of the mobile coordinate frame {A}.

Substituting Eq. (5) into Eq. (4) produces

$$\delta L_i\mathbf{u}_i + L_i\delta\mathbf{u}_i = \delta\boldsymbol{\omega}\times\mathbf{R}\mathbf{a}_i + \mathbf{R}\delta\mathbf{a}_i + \delta\mathbf{t} - \delta\mathbf{b}_i \tag{6}$$

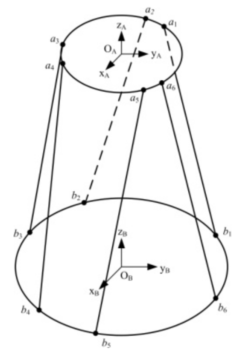

(a) Coordinate Frames

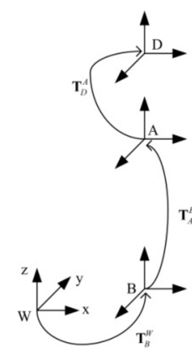

(b) The Relationships among all Transformation Matrices

Figure 2. **Schematic Diagram of a Semi-physical Simulation System.**

By multiplying $\mathbf{u}_i^T$ on both sides of Eq. (6), it can be represented as

$$\delta L_i = \begin{bmatrix}\mathbf{u}_i^T & (\mathbf{R}\mathbf{a}_i\times\mathbf{u})^T\end{bmatrix}\begin{bmatrix}\delta\mathbf{t} & \delta\boldsymbol{\omega}\end{bmatrix}^T + \begin{bmatrix}\mathbf{u}_i^T\mathbf{R} & -\mathbf{u}_i^T\end{bmatrix}\begin{bmatrix}\delta\mathbf{a}_i & \delta\mathbf{b}_i\end{bmatrix}^T \tag{7}$$

Therefore, the pose error model of the parallel manipulator can be expressed as

$$\mathbf{E} = \mathbf{J}_p\mathbf{J}_s\mathbf{e}_g \tag{8}$$

Where $\mathbf{E}$ is the pose error vector, $\mathbf{E} = [\delta\mathbf{t}\ \delta\boldsymbol{\omega}]^T$, $\mathbf{e}_g$ is geometric parameter errors of the parallel manipulator, $\mathbf{e}_g = [\delta L_1\ \delta\mathbf{a}_1\ \delta\mathbf{b}_1 \cdots \delta L_6\ \delta\mathbf{a}_6\ \delta\mathbf{b}_6]^T$.

$$\mathbf{J}_p = \begin{bmatrix}\mathbf{u}_1^T & (\mathbf{R}\mathbf{a}_1\times\mathbf{u}_1)^T \\ \vdots & \vdots \\ \mathbf{u}_6^T & (\mathbf{R}\mathbf{a}_6\times\mathbf{u}_6)^T\end{bmatrix}^{-1} \tag{9}$$

$$\mathbf{J}_s = \begin{bmatrix} 1 & -\mathbf{u}_1^T\mathbf{R} & \mathbf{u}_1^T & \cdots & 0 \\ \vdots & \vdots & & & \vdots \\ 0 & \cdots & 1 & -\mathbf{u}_6^T\mathbf{R} & \mathbf{u}_6^T \end{bmatrix} \tag{10}$$

Eq. (8) shows the actuator length errors, the upper joint position errors and the lower joint position errors play an important role in pose accuracy decreasing.

3 KINEMATIC CALIBRATION OF THE PARALLEL MANIPULATOR

AS described in section 2, $\mathbf{T}_A^B$ in Eq. (1) is imprecise, because of manufacturing and assembly errors of the parallel manipulator. For transformation matrices $\mathbf{T}_B^W$ and $\mathbf{T}_D^A$, the actual values are not provided due to the immeasurability of origins of the mobile coordinate frame {A} and the fixed coordinate frame {B}. In order to achieve their precise values, a kinematic calibration technology is established considering not only geometric parameter errors of the parallel manipulator but also the transformation errors for $\mathbf{T}_B^W$ and $\mathbf{T}_D^A$. By using the differential transformation relationship, Eq. (1) can be rewritten as

$$\mathbf{T}_D^W + d\mathbf{T}_D^W = \left(\mathbf{T}_B^W + d\mathbf{T}_B^W\right)\left(\mathbf{T}_A^B + d\mathbf{T}_A^B\right)\left(\mathbf{T}_D^A + d\mathbf{T}_D^A\right) \tag{11}$$

Removing the parentheses on the right side of Eq. (11) and neglecting the high order terms, it can be represented as

$$d\mathbf{T}_D^W = d\mathbf{T}_B^W\mathbf{T}_A^B\mathbf{T}_D^A + \mathbf{T}_B^W d\mathbf{T}_A^B\mathbf{T}_D^A + \mathbf{T}_B^W\mathbf{T}_A^B d\mathbf{T}_D^A \tag{12}$$

Basing on matrix differential theory, a matrix transformation error can be expressed as

$$d\mathbf{T} = \mathbf{T}\delta\mathbf{T} \tag{13}$$

where $\delta\mathbf{T}$ is written as

$$\delta\mathbf{T} = \begin{bmatrix} 0 & -\delta z & \delta y & dx \\ \delta z & 0 & -\delta x & dy \\ -\delta y & \delta x & 0 & dz \\ 0 & 0 & 0 & 0 \end{bmatrix} \tag{14}$$

where dx, dy, and dz are position errors, δx, δy, and δz are the orientation errors.

Substituting Eq. (13) into Eq. (12), the formula can be obtained as

$$\mathbf{T}_D^W\delta\mathbf{T}_D^W = \mathbf{T}_D^W\begin{pmatrix} \left(\mathbf{T}_A^B\mathbf{T}_D^A\right)^{-1}\delta\mathbf{T}_B^W\mathbf{T}_A^B\mathbf{T}_D^A + \\ \left(\mathbf{T}_D^A\right)^{-1}\delta\mathbf{T}_A^B\mathbf{T}_D^A + \delta\mathbf{T}_D^A \end{pmatrix} \tag{15}$$

By letting $\mathbf{U} = \mathbf{T}_A^B\mathbf{T}_D^A$ and $\mathbf{V} = \mathbf{T}_D^A$, Eq. (15) can be simplified as

$$\delta\mathbf{T}_D^W = \mathbf{U}^{-1}\delta\mathbf{T}_B^W\mathbf{U} + \mathbf{V}^{-1}\delta\mathbf{T}_A^B\mathbf{V} + \delta\mathbf{T}_D^A \tag{16}$$

It is noted that $\mathbf{U}$ and $\mathbf{V}$ can be in the form of

$$\mathbf{U} = \begin{bmatrix} \mathbf{n}_u & \mathbf{o}_u & \mathbf{a}_u & \mathbf{r}_u \\ 0 & 0 & 0 & 1 \end{bmatrix} \tag{17}$$

$$\mathbf{V} = \begin{bmatrix} \mathbf{n}_v & \mathbf{o}_v & \mathbf{a}_v & \mathbf{r}_v \\ 0 & 0 & 0 & 1 \end{bmatrix} \tag{18}$$

where $\mathbf{n}_u$, $\mathbf{o}_u$, and $\mathbf{a}_u$ are orthogonal unit vectors of $\mathbf{U}$, $\mathbf{r}_u$ is translation vector of $\mathbf{U}$, $\mathbf{n}_v$, $\mathbf{o}_v$, and $\mathbf{a}_v$ are orthogonal unit vectors of $\mathbf{V}$, $\mathbf{r}_v$ is translation vector of $\mathbf{V}$.

According to Eq. (14), $\delta\mathbf{T}_D^W$, $\delta\mathbf{T}_B^W$, $\delta\mathbf{T}_A^B$, and $\delta\mathbf{T}_D^A$ can be represented as

$$\delta\mathbf{T}_D^W = \begin{bmatrix} 0 & -\delta z & \delta y & dx \\ \delta z & 0 & -\delta x & dy \\ -\delta y & \delta x & 0 & dz \\ 0 & 0 & 0 & 0 \end{bmatrix} \tag{19}$$

$$\delta\mathbf{T}_B^W = \begin{bmatrix} 0 & -\delta z_b & \delta y_b & dx_b \\ \delta z_b & 0 & -\delta x_b & dy_b \\ -\delta y_b & \delta x_b & 0 & dz_b \\ 0 & 0 & 0 & 0 \end{bmatrix} \tag{20}$$

$$\delta\mathbf{T}_A^B = \begin{bmatrix} 0 & -\delta z_a & \delta y_a & dx_a \\ \delta z_a & 0 & -\delta x_a & dy_a \\ -\delta y_a & \delta x_a & 0 & dz_a \\ 0 & 0 & 0 & 0 \end{bmatrix} \tag{21}$$

$$\delta\mathbf{T}_D^A = \begin{bmatrix} 0 & -\delta z_d & \delta y_d & dx_d \\ \delta z_d & 0 & -\delta x_d & dy_d \\ -\delta y_d & \delta x_d & 0 & dz_d \\ 0 & 0 & 0 & 0 \end{bmatrix} \tag{22}$$

Letting $\mathbf{d}_b = \left[dx_b\ dy_b\ dz_b\right]^T$ and $\boldsymbol{\delta}_b = \left[\delta x_b\ \delta y_b\ \delta z_b\right]^T$, the triple product of matrix $\mathbf{U}^{-1}\delta\mathbf{T}_B^W\mathbf{U}$ is expressed as

$$\mathbf{U}^{-1}\delta\mathbf{T}_B^W\mathbf{U}=\begin{bmatrix}0 & -\boldsymbol{\delta}_b\cdot\mathbf{a}_u & \boldsymbol{\delta}_b\cdot\mathbf{o}_u & \boldsymbol{\delta}_b\cdot(\mathbf{r}_u\times\mathbf{n}_u)+\mathbf{d}_b\cdot\mathbf{n}_u\\ \boldsymbol{\delta}_b\cdot\mathbf{a}_u & 0 & -\boldsymbol{\delta}_b\cdot\mathbf{n}_u & \boldsymbol{\delta}_b\cdot(\mathbf{r}_u\times\mathbf{o}_u)+\mathbf{d}_b\cdot\mathbf{o}_u\\ -\boldsymbol{\delta}_b\cdot\mathbf{o}_u & \boldsymbol{\delta}_b\cdot\mathbf{n}_u & 0 & \boldsymbol{\delta}_b\cdot(\mathbf{r}_u\times\mathbf{a}_u)+\mathbf{d}_b\cdot\mathbf{a}_u\\ 0 & 0 & 0 & 0\end{bmatrix} \tag{23}$$

Similarly, letting $\mathbf{d}_a=[dx_a\ dy_a\ dz_a]^T$ and $\boldsymbol{\delta}_a=[\delta x_a\ \delta y_a\ \delta z_a]^T$, the triple product of matrix $\mathbf{V}^{-1}\delta\mathbf{T}_A^B\mathbf{V}$ is written as

$$\mathbf{V}^{-1}\delta\mathbf{T}_A^B\mathbf{V}=\begin{bmatrix}0 & -\boldsymbol{\delta}_a\cdot\mathbf{a}_v & \boldsymbol{\delta}_a\cdot\mathbf{o}_v & \boldsymbol{\delta}_a\cdot(\mathbf{r}_v\times\mathbf{n}_v)+\mathbf{d}_a\cdot\mathbf{n}_v\\ \boldsymbol{\delta}_a\cdot\mathbf{a}_v & 0 & -\boldsymbol{\delta}_a\cdot\mathbf{n}_v & \boldsymbol{\delta}_a\cdot(\mathbf{r}_v\times\mathbf{o}_v)+\mathbf{d}_a\cdot\mathbf{o}_v\\ -\boldsymbol{\delta}_a\cdot\mathbf{o}_v & \boldsymbol{\delta}_a\cdot\mathbf{n}_v & 0 & \boldsymbol{\delta}_a\cdot(\mathbf{r}_v\times\mathbf{a}_v)+\mathbf{d}_a\cdot\mathbf{a}_v\\ 0 & 0 & 0 & 0\end{bmatrix} \tag{24}$$

By using Eq. (16), (19), (22), (23) and (24), the following equations are established

$$\begin{aligned}
dx&=\boldsymbol{\delta}_b\cdot(\mathbf{r}_u\times\mathbf{n}_u)+\mathbf{d}_b\cdot\mathbf{n}_u+\boldsymbol{\delta}_a\cdot(\mathbf{r}_v\times\mathbf{n}_v)+\mathbf{d}_a\cdot\mathbf{n}_v+dx_d\\
dy&=\boldsymbol{\delta}_b\cdot(\mathbf{r}_u\times\mathbf{o}_u)+\mathbf{d}_b\cdot\mathbf{o}_u+\boldsymbol{\delta}_a\cdot(\mathbf{r}_v\times\mathbf{o}_v)+\mathbf{d}_a\cdot\mathbf{o}_v+dy_d\\
dz&=\boldsymbol{\delta}_b\cdot(\mathbf{r}_u\times\mathbf{a}_u)+\mathbf{d}_b\cdot\mathbf{a}_u+\boldsymbol{\delta}_a\cdot(\mathbf{r}_v\times\mathbf{a}_v)+\mathbf{d}_a\cdot\mathbf{a}_v+dz_d\\
\delta x&=\boldsymbol{\delta}_b\cdot\mathbf{n}_u+\boldsymbol{\delta}_a\cdot\mathbf{n}_v+\delta x_d\\
\delta y&=\boldsymbol{\delta}_b\cdot\mathbf{o}_u+\boldsymbol{\delta}_a\cdot\mathbf{o}_v+\delta y_d\\
\delta z&=\boldsymbol{\delta}_b\cdot\mathbf{a}_u+\boldsymbol{\delta}_a\cdot\mathbf{a}_v+\delta z_d
\end{aligned} \tag{25}$$

Letting $\mathbf{R}_u=[\mathbf{n}_u\quad\mathbf{o}_u\quad\mathbf{a}_u]^T$, $\mathbf{R}_v=[\mathbf{n}_v\quad\mathbf{o}_v\quad\mathbf{a}_v]^T$ $\mathbf{C}_u=[\mathbf{r}_u\times\mathbf{n}_u\quad\mathbf{r}_u\times\mathbf{o}_u\quad\mathbf{r}_u\times\mathbf{a}_u]^T$ $\mathbf{C}_v=[\mathbf{r}_v\times\mathbf{n}_v\quad\mathbf{r}_v\times\mathbf{o}_v\quad\mathbf{r}_v\times\mathbf{a}_v]^T$, $\mathbf{d}=[dx\quad dy\quad dz]^T$ $\boldsymbol{\delta}=[\delta x\quad\delta y\quad\delta z]^T$, $\mathbf{d}_d=[dx_d\quad dy_d\quad dz_d]^T$, $\boldsymbol{\delta}_d=[\delta x_d\quad\delta y_d\quad\delta z_d]^T$, Eq. (25) is written in matrix form as

$$\begin{bmatrix}\mathbf{d}\\ \boldsymbol{\delta}\end{bmatrix}=\begin{bmatrix}\mathbf{R}_u & \mathbf{C}_u & \mathbf{R}_v & \mathbf{C}_v & \mathbf{I}_{3\times3} & \mathbf{O}_{3\times3}\\ \mathbf{O}_{3\times3} & \mathbf{R}_u & \mathbf{O}_{3\times3} & \mathbf{R}_v & \mathbf{O}_{3\times3} & \mathbf{I}_{3\times3}\end{bmatrix}\begin{bmatrix}\mathbf{d}_b\\ \boldsymbol{\delta}_b\\ \mathbf{d}_a\\ \boldsymbol{\delta}_a\\ \mathbf{d}_d\\ \boldsymbol{\delta}_d\end{bmatrix} \tag{26}$$

Where $\mathbf{I}$ is the unit matrix and $\mathbf{O}$ is the zero matrix.

Substituting Eq. (8) into Eq. (26), it can be rewritten as

$$\begin{bmatrix}\mathbf{d}\\ \boldsymbol{\delta}\end{bmatrix}=\begin{bmatrix}\mathbf{R}_u & \mathbf{C}_u & \mathbf{R}_v & \mathbf{C}_v & \mathbf{I}_{3\times3} & \mathbf{O}_{3\times3}\\ \mathbf{O}_{3\times3} & \mathbf{R}_u & \mathbf{O}_{3\times3} & \mathbf{R}_v & \mathbf{O}_{3\times3} & \mathbf{I}_{3\times3}\end{bmatrix}\cdot\begin{bmatrix}\mathbf{I}_{6\times6} & \mathbf{O}_{6\times42} & \mathbf{O}_{6\times6}\\ \mathbf{O}_{6\times6} & \mathbf{J}_p\mathbf{J}_s & \mathbf{O}_{6\times6}\\ \mathbf{O}_{6\times6} & \mathbf{O}_{6\times42} & \mathbf{I}_{6\times6}\end{bmatrix}\begin{bmatrix}\mathbf{d}_b\\ \boldsymbol{\delta}_b\\ \mathbf{e}_g\\ \mathbf{d}_d\\ \boldsymbol{\delta}_d\end{bmatrix} \tag{27}$$

The calibration model given in Eq. (27) is further simplified as

$$\mathbf{x}=\mathbf{J}\mathbf{y} \tag{28}$$

where $\mathbf{x}=[\mathbf{d}\ \boldsymbol{\delta}]^T$ is a pose error vector and $\mathbf{y}=[\mathbf{d}_b\ \boldsymbol{\delta}_b\ \mathbf{e}_g\ \mathbf{d}_a\ \boldsymbol{\delta}_a]^T$ is a parameter error vector. The calibration model can be used to identify the geometrical parameter errors of the parallel manipulator and the transformation errors of $\mathbf{T}_\mathrm{B}^W$ and $\mathbf{T}_D^A$.

There are 54 parameter errors to be estimated as shown in Eq. (28), while the equations are 6. Therefore, at least 9 sets of pose measurement are required to identify 54 parameter errors. Given n sets of pose error vector, $6\times n$ calibration equations can be obtained and written in matrix form

$$\bar{\mathbf{x}}=\bar{\mathbf{J}}\mathbf{y} \tag{29}$$

where $\bar{\mathbf{x}}=[\mathbf{x}_1^T\ \mathbf{x}_2^T\cdots\mathbf{x}_n^T]^T$ is pose error matrix, $\bar{\mathbf{J}}=[\mathbf{J}_1^T\ \mathbf{J}_2^T\cdots\mathbf{J}_n^T]^T$ is parameter error identification matrix. The least squares solution for $\mathbf{y}$ is

$$\mathbf{y}=\left(\mathbf{J}^T\mathbf{J}\right)^{-1}\mathbf{J}^T\bar{\mathbf{x}} \tag{30}$$

In order to ensure that the least square solution is closer to its truth value, successive iteration algorithm can be used to identify the parameter error. The parameter errors are substituted as the correction of geometrical parameters of the parallel manipulator and transformation matrix of the coordinate. The above calculation procedure is repeated until the parameter errors are satisfied the following formula

$$-\varepsilon \le \mathbf{y}^{(k)} - y^{(k-1)} \le \varepsilon \tag{31}$$

where ε is error tolerance.

4 COMPUTER SIMULATIONS AND EXPERIMENTAL RESULTS

THE feasibility for kinematic calibration method presented in the paper was verified by computer simulations. The following hypothesis was made:

(1) The transformation matrix, $\mathbf{T}_D^A$, between the docking coordinate frame {D} and the mobile coordinate frame {A} is considered as an identity matrix before kinematic calibration. Similarly, the transformation matrix, $\mathbf{T}_\mathrm{B}^W$, between the fixed coordinate frame {B} and the world coordinate frame {W} is also an identity matrix before kinematic calibration.

(2) A set of predefined transformation errors was listed in Table 1. These errors were appended the three transformation matrices, namely, $\mathbf{T}_D^A$, $\mathbf{T}_A^B$, and $\mathbf{T}_\mathrm{B}^W$. The computation results were used as pose actual value. The transformation matrices generated by computer simulation were taken as pose nominal value and a set of actuator length was given in Table 2.

The computer simulation results of the kinematic calibration are shown in Table 3 and Figure 3. Since the kinematic calibration is an iterative computation process, the relationship between the pose error of the parallel manipulator and the number of iterations in the computer simulation and shown in Figure 3. In order to evaluate the effect of the kinematic calibration, the following two error parameters are defined: RMSPE and RMSOE, which are the root mean square position and orientation errors. From the computer simulation results above, it can be seen that the pose error of the parallel manipulator decreases gradually while the number of iteration increases, and the expected effect of kinematic calibration is obtained. The set of geometrical parameter errors and transformation errors can be identified through least squares algorithm.

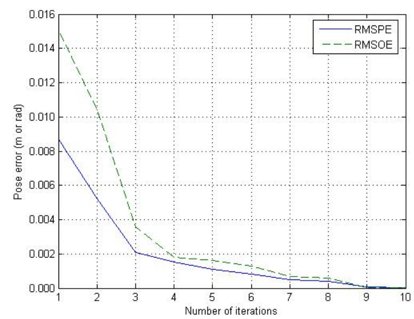

Figure 3. The Relationship between Pose Errors and Number of Iteration in a Simulation.

Table 1. Predefined Transformation Errors (m or rad).

Error matrix	dx	dy	dz	δx	δy	δz
$\mathbf{T}_\mathrm{B}^W$	0.0120	0.0170	-0.0090	0.0300	0.0200	0.0080
	-0.0087	-0.0008	-0.0068	-0.0028	-0.0115	-0.0059
	-0.0056	-0.0010	-0.0009	0.0077	-0.0092	-0.0153
	0.0016	-0.0026	0.0039	-0.0073	0.0034	-0.0036
	-0.0080	-0.0062	0.0071	-0.0019	0.0041	0.0058
$\mathbf{T}_A^B$	-0.0024	0.0032	-0.0041	0.0136	-0.0041	-0.0128
	0.0028	0.0036	-0.0044	0.0058	0.0024	-0.0146
	0.0039	0.0041	0.0066	-0.0090	-0.0015	0.0035
	0.0035	-0.0004	-0.0048	0.0107	-0.0143	0.0034
	-0.0075	0.0010	0.0055	0.0040	-0.0149	-0.0152
$\mathbf{T}_D^A$	0.0180	0.0150	-0.0050	0.0400	0.0500	0.0020

Table 2. **Parallel Manipulator Actuator Lengths of Simulation (m or rad).**

No.	l_1	l_2	l_3	l_4	l_5	l_6
1	0.8102	-0.0995	-0.1615	0.1087	0.3626	0.0029
2	-0.4840	0.2078	0.7086	-0.2386	0.0263	0.2194
3	0.1923	0.5255	-0.7958	-0.3154	-0.3114	-0.0745
4	-0.0252	0.7593	-0.2648	-0.5076	0.1803	-0.2046
5	0.7043	0.4288	0.5637	0.2584	0.3541	-0.3250
6	0.4718	-0.5827	-0.8822	-0.0575	-0.5030	-0.3210
7	-0.0784	-0.1697	-0.6500	0.4522	0.1898	0.1908
8	-0.8667	0.7838	-0.5350	-0.0356	-0.1262	-0.2065
9	0.5785	0.7504	-0.5423	-0.0852	0.3474	0.0436

Table 3. **Iterative Error Variation in Simulation (m or rad).**

No.	1	2	3	4	5	6	7	8
RMSPE	0.0087	0.0052	0.0021	0.0015	0.0011	0.0008	0.0005	0.0004
RMSOE	0.0151	0.0104	0.0036	0.0018	0.0016	0.0013	0.0007	0.0006

The kinematic calibration results of transformation matrices $\mathbf{T}_{\mathrm{B}}^{W}$, $\mathbf{T}_{A}^{B}$ and $\mathbf{T}_{D}^{A}$ are given in Table 4. From the simulation results above, the position errors of transformation matrices $\mathbf{T}_{\mathrm{B}}^{W}$, $\mathbf{T}_{A}^{B}$ and $\mathbf{T}_{D}^{A}$ can be calibrated accurately. It is shown that the orientation errors can be calibrated by the calculation of rotation matrices for transformation matrices $\mathbf{T}_{\mathrm{B}}^{W}$, $\mathbf{T}_{A}^{B}$ and $\mathbf{T}_{D}^{A}$.

The goal of the experiments is to explore the feasibility of the kinematic calibration technique proposed in Section 3 and verified through experimental studies. Two sets of pose measurement data of the 6-DOF electro-hydraulic parallel manipulator constructed in the Aerospace System Engineering Shanghai were collected by using a laser tracking measurement system. This data is fed into the kinematic calibration algorithm to provide the experimental verification. The experimental results are shown in Table 5. The first set of pose measurement data is used in the kinematic calibration. It is obvious that the position errors are less 1 mm, and the orientation errors are not more than 0.1 degree.

Since pose measurement data are inevitably contaminated by noise, more pose measurements are needed in order to improve the identification of parameter errors in the view of least squares. The relationship between the pose accuracy and the number of pose measurement is illustrated in Figure 4. As expected better pose accuracy is achieved as the number of pose measurement increases. However, very little pose accuracy can be obtained once the number of pose measurement exceeds 30 pose measurements. It should be emphasized that the parameter errors cannot be completely eliminated due to the presence of pose measurement errors.

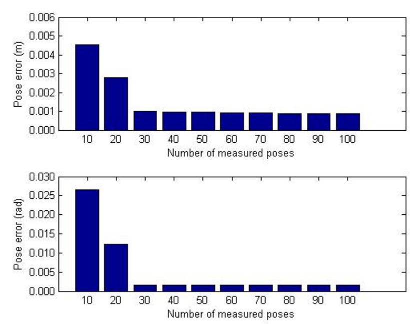

Figure 4. **The Relationship between Pose Accuracy and the Number of Pose Measurements.**

5 CONCLUSIONS

THE kinematic calibration strategy based on the laser tracking measurement method and a more complete pose error model including geometrical parameter errors of the parallel manipulator and transformation errors of the coordinate frame of the semi-physical simulation system have been proposed. The numerical values of the above errors are identified using iterative least squares algorithm. The kinematic calibration results presented in the article showed to improve the 6-DOF parallel manipulator for a semi-physical simulation system of a space docking mechanism pose accuracy to well below 1 mm and 0.1 degree.

6 DISCLOSURE STATEMENT

No potential conflict of interest was reported by the authors.

Table 4. **Simulated Calibration Results.**

Error matrix	dx	dy	dz	δx	δy	δz
$\mathbf{T}_{\mathrm{B}}^{W}$	0.0199	0.0171	-0.0089	0.0301	0.0198	0.0081
	-0.0089	-0.0009	-0.0067	-0.0029	-0.0114	-0.0060
	-0.0054	-0.0011	-0.0009	0.0079	-0.0091	-0.0152
	0.0017	-0.0027	0.0041	-0.0071	0.0036	-0.0034
	-0.0087	-0.0061	0.0072	-0.0020	0.0043	0.0059
$\mathbf{T}_{A}^{B}$	-0.0023	0.0035	-0.0039	0.0139	-0.0042	-0.0129
	0.0029	0.0038	-0.0045	0.0060	0.0027	-0.0147
	0.0040	0.0042	0.0069	-0.0089	-0.0016	0.0036
	0.0036	-0.0004	-0.0047	0.0108	-0.0141	0.0033
	-0.0073	0.0012	0.0051	0.0039	-0.0150	-0.0151
$\mathbf{T}_{D}^{A}$	0.0179	0.0151	-0.0049	0.0398	0.0509	0.0019

Table 5. **Experimental Calibration Results.**

Error Matrix	dx		dy		dz		δx		δy		δz	
	before	after	before	after	before	after	before	after	before	after	before	after
$\mathbf{T}_{\mathrm{B}}^{W}$	0.0162	0.0008	0.0090	0.0004	-0.0137	0.0007	-0.0257	-0.0014	0.0201	0.0012	-0.0112	-0.0015
	0.0020	-0.0009	0.0049	-0.0001	0.0041	-0.0009	-0.0043	-0.0010	-0.0139	0.0013	-0.0073	-0.0007
	0.0030	-0.0004	0.0039	-0.0008	0.0018	0.0006	-0.0091	0.0012	0.0073	-0.0002	-0.0003	-0.0001
	0.0002	0.0009	-0.0010	0.0001	0.0012	0.0009	-0.0121	0.0008	-0.0054	0.0007	-0.0021	0.0011
	0.0000	-0.0008	0.0013	-0.0001	0.0001	-0.0004	-0.0053	-0.0003	0.0060	-0.0015	0.0083	-0.0007
	0.0025	0.0002	-0.0011	-0.0006	-0.0050	-0.0002	-0.0046	-0.0007	-0.0117	-0.0016	0.0074	0.0007
	-0.0026	-0.0001	0.0035	-0.0007	-0.0027	0.0005	-0.0035	-0.0001	0.0097	0.0000	-0.0073	-0.0014
	0.0044	0.0004	0.0003	0.0008	0.0048	-0.0001	0.0127	-0.0012	0.0061	0.0013	0.0038	0.0009
	-0.0041	0.0007	0.0031	-0.0007	0.0036	-0.0008	0.0061	-0.0000	0.0104	0.0010	-0.0075	-0.0001
	0.0004	-0.0006	-0.0011	0.0009	-0.0049	0.0009	0.0078	0.0001	0.0104	0.0010	0.0032	0.0015
	0.0040	-0.0001	0.0046	0.0004	-0.0001	0.0001	0.0033	0.0000	0.0073	-0.0010	-0.0065	-0.0017
$\mathbf{T}_{A}^{B}$	0.0036	0.0008	-0.0047	0.0009	-0.0008	-0.0007	0.0042	-0.0009	0.0047	0.0007	0.0138	-0.0015
	0.0013	-0.0009	0.0045	0.0006	0.0027	-0.0007	0.0072	0.0015	0.0113	-0.0010	0.0073	0.0008
	-0.0024	0.0005	0.0021	-0.0009	-0.0001	0.0007	-0.0099	0.0001	0.0090	0.0010	-0.0005	0.0005
	-0.0012	0.0006	0.0015	-0.0003	0.0002	0.0004	0.0028	-0.0001	0.0093	-0.0011	0.0125	0.0015
	-0.0016	-0.0004	-0.0005	0.0001	0.0028	0.0009	0.0112	0.0009	0.0039	-0.0010	-0.0039	-0.0001
	-0.0019	-0.0005	-0.0033	-0.0004	0.0009	0.0006	-0.0092	0.0008	-0.0096	-0.0001	-0.0116	0.0000
	0.0045	-0.0001	0.0034	0.0003	-0.0037	0.0006	0.0089	0.0003	0.0079	-0.0014	0.0126	-0.0003
	0.0004	0.0004	0.0047	-0.0003	-0.0039	0.0005	-0.0121	-0.0015	0.0065	0.0003	0.0053	-0.0003
	0.0020	0.0008	-0.0037	0.0009	0.0016	0.0008	0.0128	-0.0015	0.0018	-0.0011	0.0032	-0.0004
	0.0038	-0.0001	-0.0025	-0.0003	0.0050	-0.0008	-0.0051	0.0005	0.0063	0.0015	0.0111	0.0012
$\mathbf{T}_{D}^{A}$	0.007	0.0008	0.003	0.0002	0.0128	0.0009	-0.0273	0.0013	-0.0328	-0.0016	0.0104	0.0016

7 REFERENCES

S. P. Bai & M. Y. Teo, (2003). Kinematic calibration and pose measurement of a mdical parallel manipulator by optical position sensors, *Journal of Robotic Systems*. 20(4), 201-209.

J. J. Bernhard, J. C. Ziegert, and B. Lothar, (2001). Uncertainty propagation in calibration of parallel kinematic machines, *Precision Engineering*. 25(1), 48-55.

S. Besnard & W. Khalil, (1999). Calibration of Parallel Robots Using Two Inclinometers, *Proceedings IEEE International Conference on Robotics and Automation*. 3, 1758-1763.

D. Daney, (2003). Kinematic calibration of the Gough platform, *Robotica*. 21(6), 677-690.

J. G. Li, J. Ding, Y. X. Yao, and H. G. Fang, (2015). A new accuracy design for a 6-dof docking mechanism, *Proceedings of the Institution of Mechanical Engineers, Part C. Journal Mechanical Engineering Science*. 229(18), 3473-3483.

T. M. Li, F. C. Li, Y. Jiang, J. L. Zhang, and H. T. Wang, (2017). Kinematic calibration of a 3-P(Pa)S parallel-type spindle head considering the thermal error, *Mechatronics*. 43, 86-98.

O. Masory, J. Wang, and H. Q. Zhuang, (1993). On the accuracy of a Stewart platform-part II kinematic calibration and compensation, *Proceedings IEEE International Conference on Robotics and Automation*. 1, 725-731.

A. J. Patel & K. F. Ehmann, (2000). Calibration of a hexapod machine tool using a redundant leg, *International Journal of Machine Tools and Manufacture*. 40(4), 489-512.

A. Rauf, A. Pervez, and J. Ryu, (2006). Experimental results on kinematic calibration of parallel manipulators using a partial pose measurement device, *IEEE Transaction on Robotics*. 22(2), 379-384.

X. D. Ren, Z. R. Feng, and C. P. Su, (2009). A new calibration method for parallel kinematics machine tools using orientation constraint, *International Journal of Machine Tools and Manufacture*. 49(9), 708-721.

P. Renaud, N. Andreff, J. M. Lavest, and M. Dhome, (2006). Simplifying the kinematic calibration of parallel mechanisms using vision-based metrology, *IEEE Transactions on Robotics*. 22(1), 12-22.

T. Ropponen & T. Arai, (1995). Accuracy analysis of a modified Stewart platform manipulator, *Proceedings IEEE International Conference on Robotics and Automation*. 1, 521-525.

J. Ryu & J. Cha, (2003). Volumetric error analysis and architecture optimization for accuracy of HexaSlide type parallel manipulators, *Mechanism and Machine Theory*. 38(3), 227-240.

T. Sun, Y. P. Zhai, Y. M. Song, and J. T. Zhang, (2016). Kinematic calibration of a 3-DOF rotational parallel manipulator using laser tracker, *Robotics and Computer-Integrated Manufacturing*. 41(5), 78-91.

Y. Takeda, G. Shen, and H. Funabashi, (2004). A DBB-based kinematic calibration method for in-parallel actuated mechanisms using a Fourier series, *Journal of Mechanical Design*. 126(5), 1201-1210.

W. J. Tian, F. W. Yin, H. T. Liu, J. H. Li, Q. Li, T. Huang, and D. G. Chetwynd, (2016). Kinematic calibration of a 3-DOF spindle head using a double bar, *Mechanism and Machine Theory*. 102, 167-178.

M. Verner, F. F. Xi, and C. Mechefske, (2005). Optimal calibration of parallel kinematic machines, *Journal of Mechanical Design*. 127(1), 62-69.

J. Wang & O. Masory, (1993). On the accuracy of a Stewart platform-part I the effect of manufacturing tolerances, *Proceedings IEEE International Conference on Robotics and Automation*. 1, 114-120.

S. M. Wang & K. F. Ehmann, (2002). Error model and accuracy analysis of a six-DOF Stewart platform, *Journal of manufacturing Science and Engineering*. 124(2), 286-295.

J. J. Yao, L. Zhang, S. Chen S, Z. S. Wang, T. Wang, and Q. T. Niu, (2017). Translational shaking tests achieved on a 6-DOF hydraulic parallel manipulator, *Industrial Robot*: *An International Journal*. 43(1), 103-111.

C. F. Yang, Q. T. Huang, and J. W. Han, (2012). Decoupling control for spatial six-degree-of-freedom electro-hydraulic parallel robot, *Robotics and Computer-Integrated Manufacturing*. 28(1), 14-23.

C. F. Yang, Z. Y. Qu, and J. W. Han, (2014). Decoupled-space control and experimental evaluation of spatial electro-hydraulic robotic manipulators using singular value decomposition algorithms, *IEEE Transactions on Industrial Electronics*. 61(7), 3427-3438.

H. Q. Zhuang & Z. S. Roth, (1995). A tutorial on robot calibration with hand-mounted cameras, Intelligent Automation & Soft Computing. 1(3), 325-343.

H. Q. Zhuang & J. H. Yan, (1998). Calibration of Stewart platforms and other parallel manipulators by minimizing inverse kinematic residuals, J*ournal of Robotic Systems*. 15(7), 395-405.

8 NOTES ON CONTRIBUTORS

Dayong Yu received Ph.D. degree in Mechanical Engineering at the Harbin Institute of Technology. He works at the School of Mechanical Engineering in the University of Shanghai for Science and Technology in China. He is an associate professor at this University. His research interests are in kinematic calibration and accuracy analysis of parallel manipulators.